High-efficiency squeezed light generation for gravitational wave detectors

View the article online for updates and enhancements.

AAS | **IOP** Astronomy ebooks

Part of your publishing universe and your first choice for astronomy, astrophysics, solar physics and planetary science ebooks.

iopscience.org/books/aas

High-efficiency squeezed light generation for gravitational wave detectors

M Mehmet and H Vahlbruch

Max Planck Institut für Gravitationsphysik (Albert Einstein Institut) and Institut für Gravitationsphysik der Leibniz Universität Hannover, Callinstrasse 38, 30167 Hannover, Germany

E-mail: moritz.mehmet@aei.mpg.de

Abstract

The engineering of strongly squeezed vacuum states of light is a key technology for the reduction of quantum noise in gravitational wave detectors. We report on the observation of up to 12.0 dB squeezed vacuum states of light at the wavelength of 1064 nm in the frequency band from 10 Hz to 100 kHz. This is the strongest squeezing reported to date within this detection band. The squeezed states were generated in a half-monolithic, standing-wave cavity optical parametric amplifier, which was resonant for the fundamental and harmonic light fields. We chose appropriate reflectivities to obtain a significant reduction of the required pump power, which was 8.6 mW only. Our analysis revealed that the residual measurement phase noise was smaller than 3.5 mrad rms and that the squeezed light source provided up to 14 dB of squeezing for a downstream application. The experiment was electronically stabilized in all relevant degrees of freedom, demonstrating the applicability of the linear, doubly resonant cavity topology for current and future gravitational wave detectors.

Keywords: squeezed vacuum states of light, gravitational wave detection, quantum engineering

(Some figures may appear in colour only in the online journal)

1. Introduction

The potential of using squeezed states of light [1–4] to enhance measurement processes beyond their classical limit has been demonstrated, for example, in spectroscopy experiments [5], laser-based particle tracking of living cells [6], to generate entangled quantum states for quantum-dense metrology [7] or to establish universally secure quantum key distribution [8]. The most prominent application of squeezed states of light so far is to increase the sensitivity of gravitational wave detectors, as proposed in [9] and demonstrated in GEO 600 [10] and LIGO [11]. The long term operation of a squeezing enhanced interferometer configuration has been demonstrated at GEO 600, where squeezed states have been injected continuously since 2010 [12, 13]. Both the LIGO detectors and the Virgo detector are currently working on the integration of the squeezed light technique aiming for routine operation in the upcoming observation periods. Furthermore, squeezing enhancement has become an integral part of the conceptual layout of planned third-generation detectors, such as the European Einstein Telescope [14] and the US-American Cosmic Explorer [15]. For these future generation instruments the aim is to apply squeezed states of light and achieve a level of 10 dB non-classical noise reduction to reach their envisaged sensitivities. A prerequisite for such a sensitivity enhancement is a squeezed light source that provides strongly squeezed vacuum states of light at the expected gravitational wave signal frequencies ranging from 10 Hz to 10 kHz.

Todays most efficient squeezed light sources typically employ cavity-enhanced parametric down-conversion, also called optical parametric amplification, where the interaction between the fundamental and second harmonic fields via a $\chi^{(2)}$-process inside a non-linear crystal produces non-classical photon-pair correlations that yield a reduced noise variance in a certain field quadrature. Cavity enhanced squeezed light generation can be realized with different optical topologies. At audio-band Fourier frequencies 9 dB squeezing was measured in a single resonant linear cavity design [16] and 11.6 dB was demonstrated in a doubly resonant bow-tie configuration [17]. The strongest squeezing demonstrated to date is a squeeze factor of 15 dB below the classical shot-noise limit at the wavelength of 1064 nm, but only measured at MHz frequencies [18]. The topology used therein, was a linear standing-wave, doubly-resonant cavity around a crystal made from periodically poled potassium titanyl phosphate (PPKTP). Up to 13 dB of non-classical noise suppression was measured at a wavelength of 1550 nm [19] in a similar cavity design, but again only at MHz frequencies.

Here we report on the first direct observation of a squeezed vacuum field with a noise reduction of up to 12 dB at Fourier frequencies between 10 Hz and 100 kHz. This was achieved by highly efficient squeezed light generation in a linear, doubly-resonant optical parametric amplifier at a wavelength of 1064 nm. A balanced homodyne detector was used to verify the squeezing spectra in the detection band of earthbound gravitational wave detectors. By the implementation of a coherent control scheme [20] we stabilized our setup in all relevant degrees of freedom for the generation and detection of the squeezed vacuum states, thereby demonstrating the applicability of the linear, doubly resonant cavity topology for current and future gravitational wave detectors. The required pump power to obtain the maximum squeezing level was just 8.6 mW which is a magnitude less compared to existing doubly resonant cavity designs for audio-band squeezing [17]. Low pump powers can be beneficial to mitigate aging processes related to green light exposed optical components and ease a fiber-guided pump field transfer without degradation in the maximum detectable squeezing level. Our analysis revealed that the measured squeezing level corresponds to an equivalent squeezing factor of up to 14 dB available for the injection into a gravitational wave detector with only 3.5 mrad rms of phase noise attributed to the squeezed light source operated in air.

2. Experimental setup

The schematic of the setup is illustrated in figure 1. As laser sources we employed two single-frequency continuous-wave NPRO lasers operated at a wavelength of 1064 nm. Laser 1 had an output power of 1 W. Laser 2 had an output power of 0.5 W and was phase locked with an offset-frequency of 7 MHz with respect to Laser 1 by a phase-locking loop (PLL). The required error signal was obtained by detecting the beat signal between two 1% laser beam pick-offs on PD_{PLL}. The PLL feedback was applied to Laser 2, actuating on the laser crystal temperature and piezo actuator with a bandwidth of 50 kHz. 1 mW of Laser 1 light was transmitted through a mode-cleaner ring cavity (MC1064) that provided spatio-temporal filtering of the beam to be used as the local oscillator (LO) for balanced homodyne detection (BHD). The remaining light was sent into a second-harmonic generator (SHG) to provide the 532 nm pump field needed to drive the optical parametric amplifier (OPA). A phase modulation was imprinted on the light from Laser 1 by an electro-optical modulator (EOM) operating at a frequency of 119 MHz. This phase modulation was used to derive length control signals for MC1064, SHG and also OPA. The SHG was a quasi-phase matched, single-ended standing wave cavity containing a 5 mm long non-linear crystal made from PPKTP. The cavity was defined by the curved crystal rear side and a piezo-driven coupling mirror with a power reflectivity of approximately 90% for the fundamental and an anti-reflection (AR) coating for the second-harmonic field. The rear-side of the crystal was highly reflective (HR) for both wavelengths and the flat front-side had a double AR coating. The generated second harmonic field was transmitted through a Faraday isolator to protect the SHG from back reflections. An electronically controlled, compact Mach–Zehnder interferometer was inserted in the green path for pump power stabilization and power control for adjustment of the parametric amplification factor inside the OPA.

Similar to the frequency doubling cavity, the OPA consisted of a piezo-actuated coupling mirror and a PPKTP crystal. The crystal was of dimensions 9.3 mm × 2 mm × 1 mm. The rear-face had a radius of curvature of 12 mm and was HR coated for 1064 nm and 532 nm, thus serving as the cavity end mirror. The PPKTP front side was AR coated for both wavelengths. We realized a doubly resonant OPA by choosing a coupling mirror with power reflectivities of approximately 88% at 1064 nm and 97.5% for the second harmonic field at 532 nm. The cavity round-trip length was approximately 74 mm, resulting in a free spectral range of about 4 GHz, a finesse of 243 at 532 nm (linewidth = 16 MHz) and a finesse of 47 at 1064 nm (linewidth = 86 MHz). The PPKTP crystal was carefully temperature stabilized to mK precision to ensure phase matching and co-resonance of both wavelength at the same time. The cavity length was held on resonance for the fundamental and pump laser fields via a Pound–Drever–Hall locking scheme. To generate the control signal 50% of the green pump field reflected off the OPA was detected with a photo detector (PD_{OPA}) via a beam splitter as shown in figure 1.

The frequency shifted Laser 2 served as the coherent control field for the squeezed vacuum states [20]. This field was mode matched to the fundamental mode of the OPA through its HR backside. Due to its interaction with the green pump field inside the OPA, the demodulation of the infrared coherent control field at 14 MHz (twice the offset frequency of 7 MHz) on PD_{CC2F} in reflection yields an error signal for controlling the phase of the pump beam. The noise properties of the generated squeezed vacuum states were measured with a balanced homodyne detector (BHD). To this end the squeezed field (SQZ in figure 1) was carefully overlapped on a 50:50 beam splitter with a bright local oscillator beam (LO) with 1 mW intensity. Each output field was detected on a high-quantum efficiency InGaAs p-i-n photodiode with a diameter of 500 μm. The resulting photocurrents were subtracted from each other, amplified and then fed into a spectrum analyzer (model SR785). The dim coherent control field which was transmitted through the OPA cavity (about 1 μW) and co-propagated with the squeezed field was used
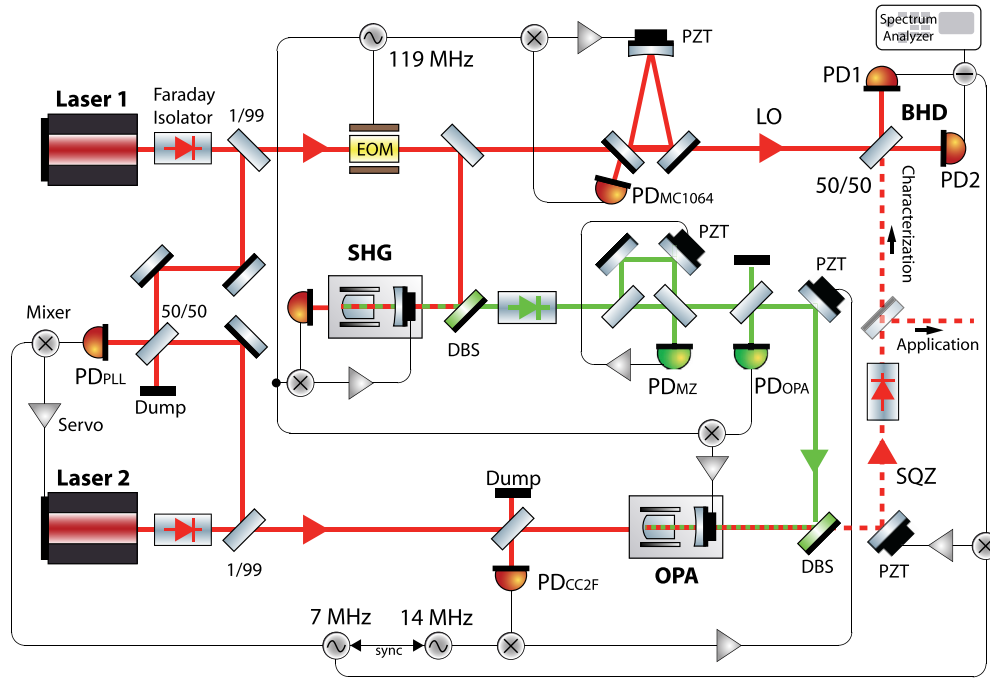
Figure 1. Schematic of the experiment. Generation and coherent control of squeezed vacuum states of light at a wavelength of 1064 nm was realized utilizing two independent but frequency offset locked laser sources. Laser 1 provided the main carrier frequency for homodyne detection and frequency doubling in a second harmonic generator (SHG), which in return provided the pump field at a wavelength of 532 nm required for the generation of squeezed vacuum states in an optical parametric amplifier (OPA) operated below threshold. The green pump power was power stabilized by a Mach–Zehnder interferometer. The squeezed vacuum states were separated from the OPA by a dichroic beamsplitter (DBS) and were subsequently characterized by means of a balanced homodyne detector (BHD). The phase of the green pump as well as the phase between the squeezed field and the LO were stabilized by the implementation of a coherent control scheme based on the 7 MHz frequency shifted Laser 2 output field. A Faraday isolator was installed in the squeezing path to protect the OPA from backscattered light.

to sense the squeezing angle at the homodyne detector. The demodulation of the detected 7 MHz beat signal and feedback to a piezo-actuated steering mirror allowed stabilization of the homodyne readout quadrature, i.e. the phase between the LO and the squeezed field. A Faraday isolator was incorporated between the squeezing resonator and homodyne detector to protect the OPA from back-reflected light which is known to introduce excess noise at audio-band Fourier frequencies due to parasitic interferences [21–23].

3. Results and discussion

Figure 2 shows various noise power spectra at Fourier frequencies between 10 Hz and 100 kHz as measured by the balanced homodyne detector. Trace (a) corresponds to the homodyne detector measurement of vacuum noise. This is the noise as measured with a 1 mW local oscillator beam and a blocked signal input port. It serves as the reference shot noise level and was carefully checked to be quantum noise limited and constant over time. All other traces

are normalized accordingly and are plotted in reference to this noise level. By injecting the generated non-classical states into the homodyne detector signal input port the output noise level changes according to the quantum noise variances of the squeezed or anti-squeezed states. For every squeezing and anti-squeezing trace shown in figure 2 the demodulation phase of the squeezing phase control loop was optimized to ensure measurement of the maximum (anti-squeezing) or minimum (squeezing) quantum noise level, respectively. A pair of traces was recorded for three different values of injected pump field power P_p at 532 nm. With $P_p = 2.8$ mW a squeeze factor of 7.0 dB below and an anti-squeeze factor of 8.0 dB above the shot noise were observed, as shown in trace (b$^-$) and trace (b$^+$), respectively. By the injection of just 6.2 mW of pump power up to 10.5 dB squeezing was measurable, see trace (c$^-$), with the corresponding anti-squeezing level of 14.2 dB above shot noise in trace (c$^+$). The maximum squeezing level, trace (d$^-$), was 12 dB obtained by injecting 8.6 mW pump power into the OPA. This is the strongest quantum noise reduction measured so far at these Fourier frequencies. The corresponding anti-squeezing level is shown in trace (d$^-$) and was measured to be 19.6 dB above the shot-noise reference. Higher levels of pump power only increased the anti-squeezing. The electronic dark noise of the homodyne detector is plotted as trace (e). It was more than 22 dB below the shot noise level at most frequencies and was not subtracted from the measurement data. Therefore all depicted squeezing values correspond to the directly observed noise suppression without any additional corrections. The squeezed ($\Delta^2 \hat{X}_-$) and anti-squeezed ($\Delta^2 \hat{X}_+$) variances of the quadrature amplitudes, produced by an OPA operated below threshold, measured at frequencies far below its bandwidth can be computed as [5]

$$\Delta^2 \hat{X}_\mp = 1 \mp \eta \frac{4\sqrt{P_p/P_{thr}}}{\left(1 \pm \sqrt{P_p/P_{thr}}\right)^2}, \tag{1}$$

where η is the total detection efficiency which depends on the optical loss ($\eta = 1 -$ total optical loss), P_p is the second-harmonic pump power injected into the OPA, and P_{thr} is the amount of pump power required to reach the oscillation threshold of the OPA. Here, the frequency dependence of the output spectra can be neglected as we are measuring at frequencies of 100 kHz and below, which is sufficiently far below the cavity linewidth of 86 MHz FWHM. For a more complete description of the measured noise spectra, in addition to optical loss one needs to take into account the influence of phase fluctuations between the signal and a quadrature phase reference. The effect of optical loss can be modeled as the addition of contributions from the unsqueezed vacuum field to the squeezed quadrature whereas phase noise couples in extra noise proportional to the anti-squeezed quadrature thereby degrading the squeezing measurement. The degradation due to phase noise increases for increasing values of P_p/P_{thr}. Therefore, low phase noise is especially important in situations with high levels of generated squeezing. If we assume the phase fluctuations to follow a Gaussian distribution with a small standard deviation, the rms phase jitter θ_{pn} of the readout quadrature corresponds to the homodyne detector measuring at an offset phase angle θ_{pn} relative to the ideal quadrature [24]. This changes the above variances according to

$$V_\mp = \Delta^2 \hat{X}_\mp \cos^2(\theta_{pn}) + \Delta^2 \hat{X}_\pm \sin^2(\theta_{pn}). \tag{2}$$

The dashed lines in figure 2 correspond to ratios $\frac{P_p}{P_{thr}}$ of 0.20, 0.47, and 0.66, assuming a total optical loss of 5.3% ($\eta = 0.947$) and a residual phase noise between homodyne signal and local oscillator field of $\theta_{pn} = 3.5$ mrad rms. The latter two parameters were assumed to be independent of $\frac{P_p}{P_{thr}}$ for the three different pairs of traces. Given the good agreement with the measurement data, the OPA threshold pump power was inferred to be just 13 mW. The slight
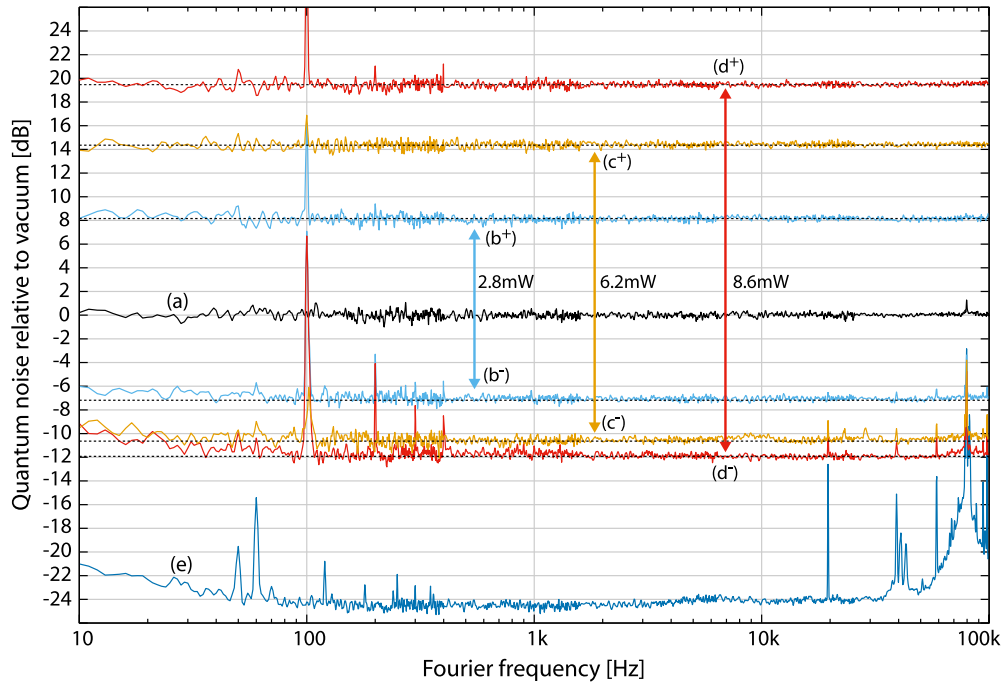
Figure 2. Quantum noise measurements performed with a balanced homodyne detector using a 1 mW intense local oscillator field. Trace (a) represents the homodyne shot noise reference measured with the signal (squeezed light) input blocked. All other traces are shown relative to this quantum noise reference. With just 2.8 mW pump power already 7 dB of squeezing and 8 dB anti-squeezing was measured as shown in trace (b⁻) and (b⁺), respectively. With an increased pump power of 6.2 mW more than 10 dB squeezing was measurable, trace (c⁻), with a corresponding anti-squeezing level of 14.2 dB shown as trace (c⁺). Trace (d⁻) and (d⁺): Up to 12 dB squeezing and 19.6 dB anti-squeezing were observed by injecting 8.6 mW into the OPA. All these measurements can be described by a theoretical model assuming a constant overall optical loss of 5.3% for the squeezed field with a fixed phase noise of 3.5 mrad rms and choosing the OPA pump parameter to be 20%, 47%, 66% of the OPA threshold, respectively. The corresponding simulations are shown as dashed lines. All measured traces are pieced together from five FFT frequency windows: 10–400 Hz, 400 Hz–1.6 kHz, 1.6–6.8 kHz, 6.8–25.2 kHz, 25.2–102.4 kHz. Each point is the averaged rms value of 200, 400, 800, 800 and 800 measurements in the respective ranges. Trace (e) is the measured homodyne detector electronic dark noise, which was not subtracted from the other data.

increase of the squeezed quantum noise at low Fourier frequencies as shown in trace (c⁻) and (d⁻), is likely due to residual stray light coupling into the system.

The measured squeeze factor was limited by optical loss which can be divided into the following contributions. The fringe visibility between the two fields at the homodyne 50/50 beamsplitter was measured to be 0.995, which corresponds to an optical loss of 1%. In independent measurements we determined the residual reflection of the non-perfect anti-reflection coating of the photodiode wafer to be 0.5% of the impinging light for each photo diode. Further loss is introduced by the imperfect quantum efficiency of the homodyne photo diodes. Without recycling of the residual reflected light we assume a quantum efficiency of approximately 99% [18]. This yields a loss contribution of 2.5% due to the homodyne measurement.

Moreover, in accordance with [18], we assign 1% of optical loss to the OPA escape efficiency and another 0.2% of loss to the propagation through non-perfectly AR-coated lenses. The Faraday isolator stage, which was constructed of two polarizing beam splitters, one half-wave plate and a Faraday rotator introduced another 1.6% optical loss for the squeezed field, adding all up to an overall loss of 5.3%, which is in a good agreement with the theoretical prediction. The residual phase noise of 3.5 mrad rms can be attributed to the laser phase locking electronics and unsuppressed noise at frequencies above unity gain of the electronic control loops.

Since the balanced homodyne detector is only needed to characterize the generated (anti-) squeezing levels one has to subtract its contribution from the optical loss budget in order to derive the squeezing degree which is available for a potential downstream application. This is depicted in figure 1 by indicating an all reflective mirror in the squeezing path, thereby bypassing the diagnostic homodyne detector. In this case the overall optical loss is reduced down to 2.8% and for a pump power of 8.6 mW our analysis reveals a squeezing level of 14 dB available for the injection into a gravitational wave detector.

4. Conclusion

In conclusion, we have reported on the direct measurement of up to 12.0 dB squeezed vacuum states at Fourier frequencies between 10 Hz and 100 kHz. This is the strongest non-classical noise suppression demonstrated in this frequency band to date. The squeezed states were produced by a highly efficient squeezed light source at a wavelength of 1064 nm employing a doubly resonant optical parametric amplifier in a standing-wave, half-monolithic cavity design. This high squeezing level was measured with a pump power of just 8.6 mW, whereas already a 7.0 dB squeezed vacuum state could be measured at a pump power of only 2.8 mW. These low levels of pump power were achieved by the simultaneous resonant enhancement of the fundamental and the second harmonic field inside the non-linear cavity. Our results agree well with a theoretical model assuming an optical loss of 5.3% including diagnostic homodyne detection and only 3.5 mrad rms phase noise. Based on the simulations we infer a maximum squeezing level of 14 dB which can be provided for a downstream application. The complete experimental setup was electronically stabilized in all required degrees of freedom and is fully compatible to current and future gravitational wave detectors.

ORCID iDs

M Mehmet ● https://orcid.org/0000-0001-9432-7108

References

[1] Yuen H P 1976 *Phys. Rev.* A **13** 2226
[2] Walls D F 1983 *Nature* **306** 141
[3] Breitenbach G, Schiller S and Mlynek J 1997 *Nature* **387** 471
[4] Schnabel R 2017 *Phys. Rep.* **684** 1–51

[5] Polzik E S, Carri J and Kimble H J 1992 *Appl. Phys.* B **55** 279
[6] Taylor M A, Janousek J, Daria V, Knittel J, Hage B, Bachor H-A and Bowen W P 2013 *Nat. Photon.* **7** 229
[7] Steinlechner S, Bauchrowitz J, Meinders M, Müller-Ebhardt H, Danzmann K and Schnabel R 2013 *Nat. Photon.* **7** 626
[8] Gehring T, Händchen V, Duhme J, Furrer F, Franz T, Pacher C, Werner R and Schnabel R 2015 *Nat. Commun.* **6** 8795
[9] Caves C M 1981 *Phys. Rev.* D **23** 1693
[10] The LIGO Scientific Collaboration 2011 *Nat. Phys.* **7** 962
[11] The LIGO Scientific Collaboration 2013 *Nat. Photon.* **8** 613
[12] Grote H, Danzmann K, Dooley K L, Schnabel R, Slutsky J and Vahlbruch H 2013 *Phys. Rev. Lett.* **110** 181101
[13] Dooley K L *et al* 2016 *Class. Quantum Grav.* **33** 075009
[14] Punturo M *et al* 2010 *Class. Quantum Grav.* **27** 084007
[15] The LIGO Scientific Collaboration 2016 *Technical Report* No. LIGO-T1600119 (https://dcc.ligo.org/T1600119/public)
[16] Vahlbruch H, Khalaidovski A, Lastzka N, Gräf Ch, Danzmann K and Schnabel R 2010 *Class. Quantum Grav.* **27** 084027
[17] Stefszky M S, Mow-Lowry C M, Chua S S Y, Shaddock D A, Buchler B C, Vahlbruch H, Khalaidovski A, Schnabel R, Lam P K and McClelland D E 2012 *Class. Quantum Grav.* **29** 145015
[18] Vahlbruch H, Mehmet M, Danzmann K and Schnabel R 2016 *Phys. Rev. Lett.* **117** 110801
[19] Schönbeck A, Thies F and Schnabel R 2018 *Opt. Lett.* **43** 110
[20] Vahlbruch H, Chelkowski S, Hage B, Franzen A, Danzmann K and Schnabel R 2006 *Phys. Rev. Lett.* **97** 011101
[21] Bowen W P, Schnabel R, Treps N, Bachor H-A and Lam P K 2002 *J. Opt. B: Quantum Semiclass. Opt.* **4** 421
[22] McKenzie K, Grosse N, Bowen W P, Whitcomb S E, Gray M B, McClelland D E and Lam P K 2004 *Phys. Rev. Lett.* **93** 161105
[23] Vahlbruch H, Chelkowski S, Danzmann K and Schnabel R 2007 *New. J. Phys.* **9** 371
[24] Aoki T, Takahashi G and Furusawa A 2006 *Opt. Express* **14** 6930